

Edge Induced Qubit Polarization in Systems with Ising Anyons

David J. Clarke and Kirill Shtengel

Department of Physics and Astronomy, University of California, Riverside, CA 92521, USA

Abstract. We investigate the proposed experimental setup for measuring the topological charge in a an Ising anyon system by means of Fabry-Pérot interferometry with a chiral edge state. We show that such an interferometer has the unintended but not necessarily unwelcome effect of stabilizing the state of the system being measured (i.e., a topological qubit). We show further that interactions between the edge mode and the localized bulk quasiparticles can have the effect of polarizing the qubit, stabilizing its state. We discuss these results in the context of recent interferometer experiments in the $\nu = 5/2$ fractional quantum Hall state, where the first of these effects is small, but the second may be relevant to the observed phenomena.

PACS numbers: 03.67.Lx, 05.30.Pr, 73.43.-f, 73.43.Jn

Submitted to: *New J. Phys.*

1. Introduction

Non-Abelian anyons are expected to occur in a number of condensed matter systems, with the most prominent example being the $\nu = 5/2$ fractional quantum Hall (FQH) state [1, 2] where some experimental evidence supports their existence [3, 4]. More recently, a slew of systems with topological superconductivity (either intrinsic or induced by a proximity effect on the boundary of a topological insulator or a semiconductor with strong spin-orbit coupling) that may support non-Abelian excitations have been proposed as well [5, 6, 7, 8]. Should non-Abelian statistics indeed be confirmed experimentally, then quantum information could potentially be stored in the combined state (fusion channel) of these quasiparticles and manipulated in a non-local, and therefore fault-tolerant, fashion [9, 10, 11]. Current proposals for measuring such quantum information involve quasiparticle interferometry [12, 13, 14, 15]. In a typical quantum Hall setting, the “arms” of a Fabry-Pérot interferometer are formed by the FQH edges, with two quantum point contacts acting as beam splitters as shown in figure 1. (Similar proposals were also adopted in the context of heterostructures of superconducting and either topologically insulating or semiconducting layers [16, 17, 18, 19].) Such a measurement scheme relies in a crucial way on the assumption that the topological charge of quasiparticles inside the interferometric loop does not change during the time required to measure it. This leads to a common concern about the feasibility of this scheme stemming from the fact that interactions between

bulk quasiparticles and the edge modes have the potential of rapidly changing the state of the bulk, which in turn will “wash out” the expected interference pattern. This makes one question even the utility of such interferometers for probing the non-Abelian nature of quasiparticle statistics, much less their reliability for storing quantum information. In other words, the question arises of how *any* interference signal might be seen in experiments like those reported by Willett et al.[3, 4] in spite of bulk-edge interactions that are estimated to be significant.

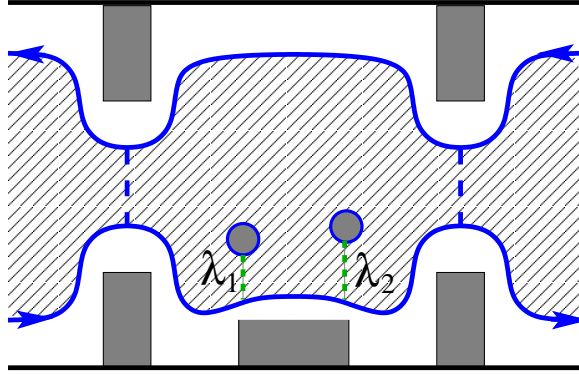


Figure 1. A typical Fabry-Pérot quasiparticle interferometer in the fractional quantum Hall setting. The interference signal results from two alternative paths taken by the probe quasiparticles entering the interferometer along the lower edge, tunnelling via one of the two quantum point contacts and leaving along the upper edge. The interference pattern depends on the fusion channel (overall topological charge) of the two localized non-Abelian anyons forming a qubit between the quantum point contacts, which in turn is affected by the coupling between these localized anyons and the edge.

It has been shown that strong quasiparticle tunnelling leads to effective absorption of quasiparticles by the edge [20, 21, 22]. However, the presence of multiple quasiparticles in the interferometric loop means that generally, some quasiparticle will be far enough away from the edge to remain unabsorbed, yet have an appreciable coupling to the edge. This would lead to the rapidly fluctuating topological charge inside the loop. The purpose of this note is to describe two additional effects that may, in principle, counter the effect of such fluctuation and lead to an observable interference signal in the presence of bulk-edge coupling.

First, a continuous measurement of the aforementioned type may have the secondary effect of stabilizing the state of the qubit being measured via the so-called “quantum Zeno effect” [23]. In Section 3, we describe the stabilizing effect of measurement in the case of coupling between two quasiparticles, one inside and another one outside the interference loop, as well as in the case of bulk-edge coupling. We demonstrate the function of the Zeno effect by analogy with a damped harmonic oscillator, and make estimates regarding the relevance of such an effect to non-Abelian interferometry experiments.

The second effect, described in Section 4, is closely related to the absorption of bulk quasiparticles by the edge as described in [20, 21, 22]. Here, we examine the case in which two quasiparticles near the same edge are both coupled to it with some strength. We find that the chiral nature of the edge and the Majorana character of

both the edge current and the bulk quasiparticles leads to a degree of polarization for the coupled quasiparticles even when they are not completely absorbed. We calculate the exact polarization as a function of the coupling strengths and temperature in the limit of a fast edge mode. In particular, we find that the polarization is greatest when the coupling strengths are comparable or when there is an energy splitting between the qubit states.

While the parameters involved in the experiments of Willett et al.[3, 4] lead us to the conclusion that an appreciable Zeno effect is unlikely, in Section 5 we estimate that a typical polarization induced by coupling of the nearest two quasiparticles to the edge may be around 16%, which in turn may explain the presence of an $e/4$ signal in these experiments despite edge-bulk interactions that would otherwise destroy it.

2. Ising anyons

The edge excitations of the Moore–Read FQH state at $\nu = 5/2$ consist of chiral bosonic excitations carrying charge $e/2$ and neutral chiral fermionic modes [24]. The non-Abelian quasiparticles carry charge $e/4$ and correspond to a twist in the boundary conditions for fermions. In the bulk these quasiparticles may be thought of as charged vortices with bound Majorana (i.e. real fermionic) zero modes. Ignoring the charge sector, these quasiparticles can be associated with (the chiral parts of) the fields I , ψ and σ appearing in the conformal field theory of the critical Ising model. The non-Abelian nature of the σ -particles is manifest in the fusion rules for the Ising spin field: $\sigma \times \sigma = I + \psi$. This translates into the statement that the combined state of two σ -particles may or may not contain a fermion.

The edge of a $p+ip$ superconductor (or, equivalently, a topological superconductor induced by a proximity effect on the surface of a topological insulator or inside a semiconductor with the strong spin-orbit coupling) lacks charge modes yet its chiral excitations can be associated with the same Ising fields, I , ψ and σ [25]. The non-Abelian anyons in this setting are unpaired Majorana modes bound to vortices [26, 27]. The complex fermion mode associated with two such excitations may be either occupied or unoccupied; these two states can span the Hilbert space of a topological qubit. Clearly, the state of such a qubit is flipped whenever a fermionic ψ -mode tunnels between the qubit and its surroundings.

For the purpose of this paper we will not distinguish between the cases with charged bosonic edge modes (FQHE) or only neutral excitations ($p + ip$ SC or its equivalents). In both cases we will loosely refer to the quasiparticles as Ising anyons despite the fact that they may differ from Ising by Abelian factors, e.g. can be obtained from Ising fields through products or cosets with $U(1)$ sectors. Importantly, in all these cases the fermionic modes remain neutral and hence their tunnelling cannot be inhibited by Coulomb energy considerations.

A real chiral fermionic edge mode is described by the Lagrangian

$$L_{\text{edge}} = \frac{i}{2} \int dx \psi (\partial_t + v \partial_x) \psi, \quad (1)$$

where the normalization has been chosen to make the fields obey the anticommutation relation

$$\{\psi(x), \psi(y)\} = 2\delta(x - y). \quad (2)$$

With this normalization,

$$\langle \psi(x)\psi(y) \rangle \sim \frac{1}{i\pi} \frac{1}{x-y} \quad (3)$$

We shall describe the localized Majorana bound states in the bulk of the system via operators γ_i such that $\gamma_i^\dagger = \gamma_i$ and

$$\{\gamma_i, \gamma_j\} = 2\delta_{ij}. \quad (4)$$

These Majorana bound states act like Ising σ fields, in that we may combine two of the bound-state operators to make a normal fermionic degree of freedom, as $\hat{f} = (\gamma_1 + i\gamma_2)/2$, so $\hat{f}^\dagger \hat{f} = (1 + i\gamma_1\gamma_2)/2$ has eigenvalues 0 and 1. In this basis, $i\gamma_1\gamma_2$ has eigenvalues of ± 1 and acts as a Pauli matrix $\sigma_z \equiv i\gamma_1\gamma_2$.

3. Zeno effect

Consider a system in which a qubit consisting of two Majorana bound states γ_1 and γ_2 accumulates error via interaction with a separate Majorana mode. The qubit can take two states corresponding to the eigenvalues of $\sigma_z = i\gamma_1\gamma_2$. We note two distinct forms of the error Hamiltonian relevant to measurements in systems with a chiral Majorana edge. First, the qubit system may interact with a localized defect outside the interferometric loop. Second, the qubit may interact with an edge. These two cases show qualitatively different behaviour.

In either case the error Hamiltonian is of the form $H_{\text{err}} = i\lambda\gamma_2\xi$, where ξ is a Majorana operator that may either be associated with a Majorana bound state or with a Majorana edge. The σ_z eigenvalue of the qubit shall be continuously measured either by environmental interactions or by an experimental apparatus in which the result of the measurement is a priori unknown. We therefore shall average over that result in our simple description.

The density matrix of the system is then governed by the equation

$$\dot{\rho}(t) = -i[H_{\text{err}}, \rho(t)] - \frac{\kappa}{4} [\sigma_z, [\sigma_z, \rho(t)]], \quad (5)$$

where κ characterizes the strength of the measurement. It shall be convenient for our analysis to consider an auxiliary variable $\bar{\rho} = e^{\kappa t} \rho(t)$, in terms of which Eq. 5 becomes:

$$\dot{\bar{\rho}}(t) = -i[H_{\text{err}}, \bar{\rho}(t)] - \frac{\kappa}{4} [\sigma_z, [\sigma_z, \bar{\rho}(t)]] + \kappa \bar{\rho}(t). \quad (6)$$

If we wish to know the qubit polarization $z = \text{Tr}(\sigma_z \rho(t))$, we can note that

$$\dot{z} = e^{-\kappa t} \text{Tr}(\sigma_z (\dot{\bar{\rho}} - \kappa \bar{\rho})) \quad (7)$$

in order to find

$$\begin{aligned} \dot{z}(t) &= e^{-\kappa t} \text{Tr}(-i[\sigma_z, H_{\text{err}}(t)] \bar{\rho}(t)) \\ &= -2 \int_0^t dt' e^{-\kappa(t-t')} \text{Tr}(\{H_{\text{err}}(t), H_{\text{err}}(t')\} \sigma_z \rho(t')) \\ &\quad + ie^{-\kappa t} \text{Tr}([\sigma_z, H_{\text{err}}(t)] \rho(0)), \end{aligned} \quad (8)$$

where we have used the cyclic nature of the trace and the fact that $\{\sigma_z, H_{\text{err}}\} = 0$.

We consider two forms for the extra Majorana mode interacting with the qubit. In the first case, $\xi = \gamma_3$ is simply a third localized Majorana state. In this case, we can map $i\gamma_2\xi \rightarrow \sigma_y$ to find

$$\begin{aligned}\dot{z}(t) &= -4\lambda^2 \int_0^t dt' e^{-\kappa(t-t')} z(t') + 2\lambda e^{-\kappa t} \text{Tr}(\sigma_x \rho(0)) \\ 0 &= \ddot{z} + \kappa \dot{z} + 4\lambda^2 z.\end{aligned}\tag{9}$$

This simple harmonic oscillator equation shows the basic function of the Zeno effect. The measurement strength acts as a drag term on the oscillator, so that as $\kappa \rightarrow \infty$, the quantum dynamics of the system is frozen (i.e. $\dot{z} = 0$).

On the other hand, for a qubit coupled to an edge $\xi = l_0^{1/2} \int dx f(x) \psi(x - vt)$, where l_0 is the short range cutoff of the theory (the magnetic length, in the quantum Hall setting) and where the edge Majorana mode ψ is governed by the Lagrangian given in (1) and obeys the anticommutation relation $\{\psi(x), \psi(y)\} = 2\delta(x - y)$. We have then that

$$\dot{z}(t) = -4\lambda^2 l_0 \int_0^t dt' e^{-\kappa(t-t')} \int dx f(x) f(x - v(t-t')) z(t'), \tag{10}$$

where we assume that the edge is in thermal equilibrium at $t = 0$, so $\text{Tr}([\sigma_z, H_{\text{err}}(t)] \rho(0)) \propto \langle \psi(x - vt) \rangle = 0$.

Importantly, if the qubit interacts with only a single point on the edge (i.e. $f(x) = \delta(x)$) then the above equation reduces to

$$\dot{z} = -2 \frac{\lambda^2 l_0}{v} z \tag{11}$$

There is no Zeno effect here due to the measurement of the qubit. Instead of oscillating, the qubit undergoes a simple decay, which does not allow the measurement time to affect the qubit.

We can relate these two cases by including a finite interaction range in the error Hamiltonian H_{err} . A particularly simple choice for the form factor of the interaction is $f(x) = (\pi a)^{-1} K_0(|x|/a)$.[‡] In this case, we have

$$\begin{aligned}\dot{z}(t) &= -\frac{2\lambda^2 l_0}{a} \int_0^t dt' e^{-(\kappa+v/a)(t-t')} z(t') \\ 0 &= \ddot{z} + \left(\kappa + \frac{v}{a}\right) \dot{z} + \frac{2\lambda^2 l_0}{a} z.\end{aligned}\tag{12}$$

Note that this reduces to the previous case (9) when the edge mode velocity tends to zero.

Using the above equation, however, we can see that the Zeno effect is likely to have limited influence in interferometric experiments of Willett et al. [3, 4]. Using parameters relevant to these experiments, the Zeno parameter κ is at most $\delta I^2/8S \sim \delta I/4e$, where $\delta I = I_0 \Delta R_{xx}/R_{xy}$, is the portion of the signal current coming from the tunnelling of $e/4$ quasiparticles and S is the spectral density of this current. With $\Delta R_{xx} = 2\Omega$, $I_0 = 2\text{nA}$ and $R_{xy} = 2h/5e^2$, this is only 604kHz, whereas the decay from edge motion is around $v/a \gtrsim v/L \sim 22\text{GHz}$ at the least, given a side length of $L = 0.45\mu\text{m}$ for the interferometer and a neutral edge velocity of $v = 10000\text{m/s}$. The Zeno effect is thus insignificant in the Willett et al. experiment, and would be for any such $nu = 5/2$ FQHE interferometer unless the size of the signal current is significantly increased.

[‡] This may be thought of as a tractable approximation to the more realistic $f(x) \propto e^{-\sqrt{(d^2+x^2)/a^2}}$, where d is the distance from the Majorana bound state to the edge.

4. Edge induced polarization

We now expand our analysis to include two Majorana bound states γ_1 and γ_2 forming a qubit that both interact with the edge at different points x_1 and x_2 . For simplicity, we shall assume a δ -like interaction with the edge. The interaction picture Hamiltonian is given by

$$H(t) = -i\lambda_1\gamma_1\psi(x_1 - vt) - i\lambda_2\gamma_2\psi(x_2 - vt). \quad (13)$$

Note that we have absorbed the short range cutoff l_0 into the definitions of λ_1 and λ_2 , which now have units of $\sqrt{\text{length}}/\text{time}$. For compactness of notation, we define $\psi_i(t) = \psi(x_i - vt)$. Equation (8) then becomes

$$\begin{aligned} \dot{z} = & -2 \frac{\lambda_1^2 + \lambda_2^2}{v} z \\ & + 2i\lambda_1\lambda_2 \int_0^t dt_1 e^{-\kappa(t-t_1)} \text{Tr} \left(([\psi_1(t), \psi_2(t_1)] - [\psi_2(t), \psi_1(t_1)]) \rho(t_1) \right). \end{aligned} \quad (14)$$

Because an interferometric measurement of this system is made using σ quasiparticles moving at the same neutral velocity v as the edge Majoranas, the actual expectation value that appears in the result of such a measurement is not z but rather

$$\tilde{z}(t) = \langle i\gamma_1(t)\gamma_2(t + \Delta x/v) \rangle = \text{Tr}(i\gamma_1(0)\gamma_2(\Delta x/v)\rho(t)), \quad (15)$$

where $\gamma_i(t) = U^\dagger(t)\gamma_i U(t)$ and $U(t) = T_{\leftarrow} \exp \left(-i \int_0^t dt' H(t') \right)$. (T_{\leftarrow} indicates time ordering with time increasing to the left). However, the time scale $\Delta x/v$ is generally significantly shorter than other experimentally relevant timescales. For simplicity in our estimates of the polarization effect, we take $\Delta x/v \rightarrow 0$ in our final result. This fast-edge approximation also allows us to disregard the fermion parity of the edge inside the interferometric loop (as treated, e.g., in [22]), as fermions leaving the qubit interaction area will also immediately leave the area of the interferometer.

Repeated application of equations (2) and (5), along with the fact that $x_2 > x_1$, allows us to set up recursion relations for the trace terms of the type in Eq. (14). For example,

$$\begin{aligned} \int_0^t dt_1 e^{-\kappa(t-t_1)} h(t-t_1) \text{Tr} \left([\psi_1(t), \psi_1(t_1)] \rho_I(t_1) \right) = \\ \int_0^t dt_1 e^{-\kappa(t-t_1)} f(t-t_1) \langle [\psi_1(t), \psi_1(t_1)] \rangle, \end{aligned} \quad (16)$$

where $h(t-t_1) = f(t-t_1) + \frac{2\lambda_1^2}{v} \int_{t_1}^t f(t-t')$. (For a full derivation of this type, see the Appendix.) Solving the resulting integral equations leads to the following expression for z :

$$\begin{aligned} \dot{z} = & -2 \frac{\lambda_1^2 + \lambda_2^2}{v} z + 2i\lambda_1\lambda_2 \left\{ \int_0^t du e^{-\kappa u} \left[e^{-\frac{2\lambda_2^2 u}{v}} g\left(u + \frac{\Delta x}{v}\right) - e^{-\frac{2\lambda_1^2 u}{v}} g\left(u - \frac{\Delta x}{v}\right) \right] \right. \\ & + \Theta\left(t - \frac{\Delta x}{v}\right) \frac{2\lambda_1^2}{\lambda_2^2 - \lambda_1^2} \int_0^{t-\Delta x/v} du \left[e^{-\left(\kappa + \frac{2\lambda_2^2}{v}\right)u} - e^{-\left(\kappa + \frac{2\lambda_1^2}{v}\right)u} \right] g\left(u + \frac{\Delta x}{v}\right) \\ & \left. - \Theta\left(t - \frac{\Delta x}{v}\right) \frac{4\lambda_1^2}{v} \int_0^{\Delta x/v} du_1 \int_{\Delta x/v}^t du_2 e^{-\left(\kappa + \frac{2\lambda_1^2}{v}\right)(u_1+u_2-\frac{\Delta x}{v})} g(u_2 - u_1) \right\} \end{aligned} \quad (17)$$

where $g(u) = \langle [\psi(-vu), \psi(0)] \rangle$ and $\Theta(x)$ is a Heaviside step function. As $t \rightarrow \infty$, the polarization z reaches an equilibrium value of

$$z_\infty = \frac{i\lambda_1\lambda_2v}{\lambda_2^2 - \lambda_1^2} \int_0^\infty du \left(e^{-(\kappa+2\lambda_2^2/v)u} - e^{-(\kappa+2\lambda_1^2/v)u} \right) g(u + \Delta x/v) \\ + \frac{\kappa}{(\kappa + 2\lambda_1^2/v)} \frac{i\lambda_1\lambda_2v}{\lambda_1^2 + \lambda_2^2} \int_{-\infty}^\infty du e^{-(\kappa+2\lambda_1^2/v)|u|} g(u + \Delta x/v), \quad (18)$$

where we have used that $g(-u) = -g(u)$. In the experimentally relevant limit $\kappa \ll 2\lambda_2^2/v$, we have

$$z_\infty = \frac{i\lambda_1\lambda_2v}{\lambda_2^2 - \lambda_1^2} \int_0^\infty du \left(e^{-2\lambda_2^2u/v} - e^{-2\lambda_1^2u/v} \right) g(u + \Delta x/v). \quad (19)$$

In the limit of small $\Delta x/v$ we may take $g(u) = 2i/\pi vu$ to find:[§]

$$z_\infty = -\frac{2\lambda_1\lambda_2}{\pi(\lambda_2^2 - \lambda_1^2)} \ln \frac{\lambda_1^2}{\lambda_2^2} \quad (20)$$

This result is dependent only on the ratio λ_1/λ_2 of the coupling constants, rather than their magnitude. However, the relaxation time for the system is $(2\lambda_1^2/v + 2\lambda_2^2/v)^{-1}$, so Majorana bound states that are only weakly coupled to the edge would require a long time to reach this equilibrium. It is interesting to note that the highest polarization allowed for two Majorana bound states that interact only through the edge in this way is $2/\pi$. This happens to be the correlation between two adjacent Majorana fermions on the edge in the discrete model of this system put forward by Rosenow et al. [22].

In order to obtain a higher degree of polarization, we must allow for an energy splitting between the two possible qubit states. A Hamiltonian term of the form $H_\epsilon = \epsilon \sigma_z/2 = i\epsilon\gamma_1\gamma_2/2$ may be induced either by interaction between the bound states γ_1 and γ_2 (see e.g. [28, 29, 30]) or by a non-locally generated energy splitting do to the circulating current of σ -quasiparticles around the edge of the interferometer, as in [31, 32]. Adding this term to the Hamiltonian (13) and repeating the above analysis (leaving $\kappa = 0$ for simplicity and taking $\Delta x/v \rightarrow 0$ as before), we obtain the more general form

$$z_\infty = -\frac{2\eta}{\pi\sqrt{\eta^2 - 1}} \arctan \sqrt{\eta^2 - 1}, \quad (21)$$

where $\eta = (v\epsilon + 2\lambda_1\lambda_2) / (\lambda_1^2 + \lambda_2^2)$. This reduces to (20) for $\epsilon = 0$.

5. Possible experimental relevance

In the experiments [3, 4] of Willett et al., the $\nu = 5/2$ plateau is found at 6.5 Tesla, corresponding to a magnetic length $l_0 = \sqrt{\hbar/(eB)} \sim 10\text{nm}$. The area of the interference loop is altered by changing a side gate voltage. Because the relevant interference occurs between edge modes with charge $e/4$, the areal change corresponding to one oscillation is $4\hbar/eB$, whereas the length of the edge containing the side gate is $0.45\mu\text{m}$. There are approximately six oscillations in each run of $e/4$ periods, corresponding to a distance between quasiparticles of approximately $d \approx 34\text{nm}$. From the numerical calculations of Baraban et al. [28], we expect the energy scale for tunnelling at this distance to be $E_1 \sim \exp[-(d - l_0)/2.3l_0] \text{K} \approx 350\text{mK}$.

[§] A result of a similar form was obtained by Rosenow et al. [20] for bulk Majoranas coupled to opposite edges of the interferometer.

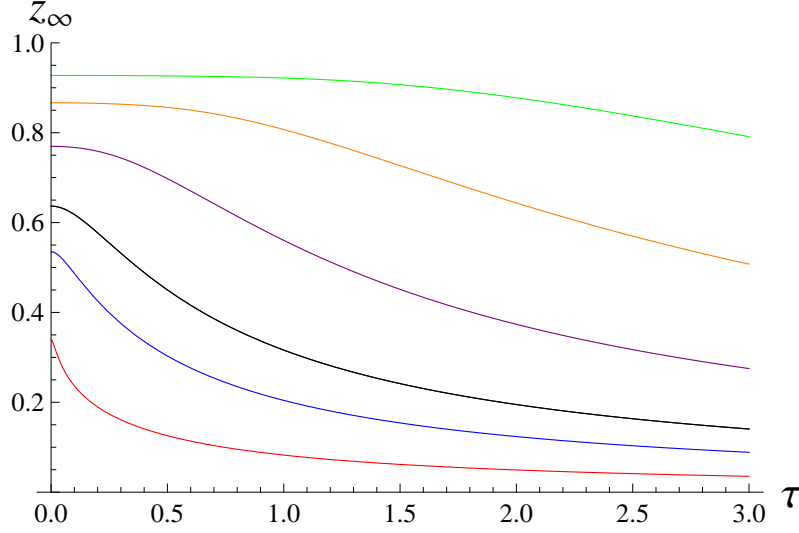


Figure 2. The equilibrium polarization due to tunnelling between two bulk Majorana bound states and the edge is plotted against the reduced temperature $\tau = \pi v T / (\lambda_1^2 + \lambda_2^2)$, where $kT_i = 2\hbar\lambda_i^2/v$, and λ_1 is the stronger bulk-edge coupling. The series of lines represent different values of $|\eta|$: 0.25 (lowest polarization, red curve), 0.63 (estimated experimental value, blue curve), 1.0 (largest attainable polarization without direct coupling between the bound states, black curve), 2.0, 4.0, and 8.0 (highest, green curve). The polarization saturates at $T = 0$ for $\eta = \mp 1$ at a value of $\pm 2/\pi$, and for $\eta = \mp \infty$ at a value of ± 1 . (Colour online).

The neutral edge velocity is of order 10^4 m/s, so this corresponds to a decay rate of roughly $2\lambda_1^2/v = 2E_1^2 l_0/v \sim 4\text{GHz}$ for the closest quasiparticle to the edge and $2\lambda_2^2/v = 2E_2^2 l_0/v \sim 0.5\text{GHz}$ for the second closest quasiparticle, which we expect to be at most around 70nm from the edge.

Note that since $v/\Delta x \gtrsim v/L \sim 22\text{GHz}$, as calculated in Sec. 3, these numbers justify the approximation $2\Delta x \lambda_i^2/v^2 \rightarrow 0$ that we have used above.

We expect then that $\lambda_1^2/\lambda_2^2 \sim 8$ and take $\epsilon = 0$, in which case the (20) leads to a polarization of approximately 52% at $T = 0$. However, the experiment of Willett et al. is conducted at a temperature of $T = 25\text{mK}$. For a finite temperature, we must replace the edge correlation function $g(u) = 2i/\pi v u$ with $g(u, T) = 2iT/[v \sinh(\pi T u)]$. The resulting polarization has the form $z = z(\eta, \tau)$ where $\eta = (v\epsilon + 2\lambda_1\lambda_2)/(\lambda_1^2 + \lambda_2^2)$ as before and $\tau = \pi v T / (\lambda_1^2 + \lambda_2^2)$:

$$z_\infty(\eta, \tau) = -\frac{i\eta}{\pi\sqrt{\eta^2 - 1}} \left[\Psi\left(\frac{\pi\tau + 1 - i\sqrt{\eta^2 - 1}}{2\pi\tau}\right) - \Psi\left(\frac{\pi\tau + 1 + i\sqrt{\eta^2 - 1}}{2\pi\tau}\right) \right], \quad (22)$$

where $\Psi(x)$ is the digamma function. (See Appendix for technical details leading to this result.) In figure 2, z_∞ is plotted as a function of the reduced temperature τ for various values of η . For the experimental values discussed above, at a temperature of $T = 25\text{mK}$, we have $|\eta| \approx 0.63$ and $\tau \approx 2.5$. This leads finally to a polarization of $\sim 16\%$.

Interestingly, the degree of polarization can be quite high if $\epsilon \gg \lambda_{1,2}^2/v$ (e.g., for

quasiparticles that are close together and far from the edge) although the relaxation time for reaching this equilibrium value is still $\sim v/\lambda^2$. In particular, the polarization can exceed $2/\pi$ provided that the two quasiparticles interact with one another inducing a non-zero energy splitting ϵ . Likewise, for non-zero ϵ , the polarization persists even if only one quasiparticle is coupled directly to the edge.

6. Discussion

In this note, we have examined two possible mechanisms for the presence of a non-Abelian signal in Ising-type anyonic interferometry despite the coupling of the Majorana bound states comprising the qubit to the edge. The first of these, the quantum Zeno effect, is in principle present in any such system due to the continuous measurement. However, as we have shown, it does not provide a viable explanation for the experimental data reported in [3, 4] due to the small value of the measurement strength parameter κ as compared with the frequency at which the edge states travel around the interferometric loop.

The second mechanism, that of qubit polarization due to the coupling of multiple bulk Majorana bound states to the edge, is more likely to explain the observed data. This mechanism is complementary to the results of Rosenow et al. [20, 22] and Bishara and Nayak [21], which describe the effective absorption of bulk Majorana states by the edge as the coupling is increased. Here, we have demonstrated that even when a pair of quasiparticles are not fully absorbed their interaction with the edge can cause a significant polarization of the qubit. This polarization is maximized when the coupling constants have equal magnitude and at $T = 0$ depends only on their ratio. We estimate, based on the parameters relevant to experiments [3, 4], that the qubit polarization may be as high as 16% when the quasiparticles are coupled to the same edge. This is significantly higher than the polarization caused by coupling to opposite edges, as found in [20]. An extension of this result to the more realistic situation of many quasiparticles in the bulk shall be the subject of future research.

Acknowledgments

The authors are grateful to A. Korotkov and S. Simon for helpful discussions. DC and KS are supported in part by the DARPA-QuEST program. KS is supported in part by the NSF under grant DMR-0748925.

Appendix

We begin with the Hamiltonian

$$H(t) = H_\lambda + H_\epsilon = -i\lambda_1\gamma_1\psi_1(t) - i\lambda_2\gamma_2\psi_2(t) + \frac{\epsilon}{2}\sigma_z, \quad (\text{A.1})$$

where $\sigma_z = i\gamma_1\gamma_2$ and $\psi_i(t) = \psi(x_i - vt)$. For simplicity, we assume the measurement parameter, κ may be safely set to 0. We set $\tilde{\rho} = e^{i\epsilon\sigma_z t/2}\rho(t)e^{-i\epsilon\sigma_z t/2}$, and $\tilde{H} = e^{i\epsilon\sigma_z t/2}H_\lambda(t)e^{-i\epsilon\sigma_z t/2} = H_\lambda(t)e^{-i\epsilon\sigma_z t}$. Then

$$\dot{\tilde{\rho}}(t) = -i[\tilde{H}(t), \tilde{\rho}(t)] \quad (\text{A.2})$$

so

$$\begin{aligned}
\dot{z}(t) &= \text{Tr}(\sigma_z \rho) = -2 \int_0^t dt_1 \text{Tr} \left(\left\{ \tilde{H}(t), \tilde{H}(t_1) \right\} \sigma_z \tilde{\rho}(t_1) \right) \\
&= -2 \int_0^t dt_1 \text{Tr} \left(\{H_\lambda(t), H_\lambda(t_1)\} \sigma_z \tilde{\rho}(t_1) \right) \cos \epsilon(t - t_1) \\
&\quad - 2i \int_0^t dt_1 \text{Tr} \left([H_\lambda(t), H_\lambda(t_1)] \tilde{\rho}(t_1) \right) \sin \epsilon(t - t_1) \\
&= -2 \frac{\lambda_1^2 + \lambda_2^2}{v} z(t) - \Theta \left(t - \frac{\Delta x}{v} \right) \frac{4\lambda_1 \lambda_2}{v} \sin \frac{\epsilon \Delta x}{v} z \left(t - \frac{\Delta x}{v} \right) \\
&\quad + 2i\lambda_1 \lambda_2 \int_0^t dt_1 \text{Tr} \left(\left([\psi_1(t), \psi_2(t_1)] - [\psi_2(t), \psi_1(t_1)] \right) \tilde{\rho}(t_1) \right) \cos \epsilon(t - t_1) \\
&\quad - 2i \int_0^t dt_1 \text{Tr} \left(\left(\lambda_1^2 [\psi_1(t), \psi_1(t_1)] + \lambda_2^2 [\psi_2(t), \psi_2(t_1)] \right) \tilde{\rho}(t_1) \right) \sin \epsilon(t - t_1),
\end{aligned} \tag{A.3}$$

where we have used that $\{\psi(x), \psi(y)\} = 2\delta(x - y)$ and the fact that $x_2 > x_1$.

We now note that for any function $f(t)$, we have that

$$\begin{aligned}
\int_0^t dt_1 f(t - t_1) \text{Tr}([\psi_i(t), \psi_j(t_1)] \tilde{\rho}(t_1)) &= \int_0^t dt_1 f(t - t_1) \langle [\psi_i(t), \psi_j(t_1)] \rangle \\
&\quad - \int_0^t dt_1 \int_0^{t_1} dt_2 \int_0^{t_2} dt_3 f(t - t_1) \text{Tr}(X_{ij}(t, t_1, t_2, t_3) \tilde{\rho}(t_3)),
\end{aligned} \tag{A.4}$$

where

$$\begin{aligned}
X_{ij} &= \left[[\psi_i(t), \psi_j(t_1)], \tilde{H}(t_2) \right], \tilde{H}(t_3) \Big] \\
&= \sum_{k,l} \lambda_k \lambda_l \left(\{ [[\psi_i(t), \psi_j(t_1)], \psi_k(t_2)], \psi_l(t_3) \} \right. \\
&\quad \times (\delta_{kl} \sin \epsilon(t_2 - t_3) - \varepsilon_{kl} \cos \epsilon(t_2 - t_3)) i\sigma_z \\
&\quad + [[[\psi_i(t), \psi_j(t_1)], \psi_k(t_2)], \psi_l(t_3)] \\
&\quad \times (\delta_{kl} \cos \epsilon(t_2 - t_3) + \varepsilon_{kl} \sin \epsilon(t_2 - t_3)) \Big),
\end{aligned} \tag{A.5}$$

where we have used that $\{\gamma_k, \gamma_l\} = 2\delta_{kl}$ and $[\gamma_k, \gamma_l] = -2i\varepsilon_{kl}\sigma_z$, where ε_{kl} is the rank 2 antisymmetric tensor.

We may now use the anticommutation relation $\{\psi_i(t), \psi_j(t')\} = 2\delta(x_i - x_j - v(t - t'))$ to note that

$$\begin{aligned}
\{ [[\psi_i(t), \psi_j(t_1)], \psi_k(t_2)], \psi_l(t_3) \} &= 8\delta(x_i - x_l - v(t - t_3)) \delta(x_j - x_k - v(t_1 - t_2)) \\
&\quad - 8\delta(x_i - x_k - v(t - t_2)) \delta(x_j - x_l - v(t_1 - t_3))
\end{aligned} \tag{A.6}$$

and

$$\begin{aligned}
&[[[\psi_i(t), \psi_j(t_1)], \psi_k(t_2)], \psi_l(t_3)] \\
&= 4[\psi_i(t), \psi_l(t_3)] \delta(x_j - x_k - v(t_1 - t_2)) - 4[\psi_j(t), \psi_l(t_3)] \delta(x_i - x_k - v(t - t_2))
\end{aligned} \tag{A.7}$$

Inserting these identities into (A.4) and using the fact that $x_2 > x_1$ leads to the general formula

$$\sum_{ij} \int_0^t dt' h_{ij}(t - t') \text{Tr}([\psi_i(t), \psi_j(t')] \tilde{\rho}(t')) = \sum_{ij} \int_0^t dt' f_{ij}(t - t') \langle [\psi_i(t), \psi_j(t')] \rangle \tag{A.8}$$

in the limit as $(x_2 - x_1)/v \rightarrow 0$, where for general functions f_{ij} we have

$$h_{i1}(t-t') = f_{i1}(t-t') + \int_{t'}^t dt_1 \left\{ \frac{2\lambda_1^2}{v} (f_{i1}(t-t_1) + 2f_{i2}(t-t_1)) \cos \epsilon(t_1-t') \right. \\ \left. - \frac{2\lambda_1\lambda_2}{v} f_{i2}(t-t_1) \sin \epsilon(t_1-t') \right\} \quad (\text{A.9})$$

and

$$h_{i2}(t-t') = f_{i2}(t-t') + \int_{t'}^t dt_1 \left\{ \frac{2\lambda_1\lambda_2}{v} (f_{i1}(t-t_1) + 2f_{i2}(t-t_1)) \sin \epsilon(t_1-t') \right. \\ \left. + \frac{2\lambda_2^2}{v} f_{i2}(t-t_1) \cos \epsilon(t_1-t') \right\}. \quad (\text{A.10})$$

We may now make the connection with the original equation (A.3) for z in the limit $t \rightarrow \infty$, $(x_2 - x_1)/v \rightarrow 0$ to find

$$z_\infty = \frac{iv}{\lambda_1^2 + \lambda_2^2} \sum_{ij} \int_0^\infty dt' f_{ij}(t') \langle [\psi_i(t'), \psi_j(0)] \rangle. \quad (\text{A.11})$$

where we now have fixed f_{ij} according to equations (A.9) and (A.10) with

$$\begin{aligned} h_{11}(t-t') &= -\lambda_1^2 \sin \epsilon(t-t') \\ h_{12}(t-t') &= \lambda_1\lambda_2 \cos \epsilon(t-t') \\ h_{21}(t-t') &= -\lambda_1\lambda_2 \cos \epsilon(t-t') \\ h_{22}(t-t') &= -\lambda_2^2 \sin \epsilon(t-t') \end{aligned} \quad (\text{A.12})$$

In the limit $(x_2 - x_1)/v \rightarrow 0$, $\langle [\psi_i(t), \psi_j(0)] \rangle = 2iT / [v \sinh(\pi T t)]$ independent of i and j . Hence, we need only the function $F(t) = \sum_{ij} f_{ij}(t) / (\lambda_1^2 + \lambda_2^2)$, which obeys the fourth order differential equation

$$(\partial_t^2 + \epsilon^2) \left[\partial_t^2 + \frac{2(\lambda_1^2 + \lambda_2^2)}{v} \partial_t + \left(\epsilon + \frac{2\lambda_1\lambda_2}{v} \right)^2 \right] F = 0 \quad (\text{A.13})$$

with

$$\begin{aligned} F(0) &= 0 \\ \partial_t F(0) &= - \left(\epsilon + \frac{2\lambda_1\lambda_2}{v} \right) \\ \partial_t^2 F(0) &= \frac{2(\lambda_1^2 + \lambda_2^2)}{v} \left(\epsilon + \frac{2\lambda_1\lambda_2}{v} \right) \\ \partial_t^3 F(0) &= \left[\left(\epsilon + \frac{2\lambda_1\lambda_2}{v} \right)^2 - \left(\frac{2(\lambda_1^2 + \lambda_2^2)}{v} \right)^2 \right] \left(\epsilon + \frac{2\lambda_1\lambda_2}{v} \right) \end{aligned} \quad (\text{A.14})$$

Remarkably, these boundary conditions lead to a relatively simple form for F :

$$F(t) = \frac{i\sqrt{-\omega_+\omega_-}}{\omega_- - \omega_+} (e^{i\omega_+t} - e^{i\omega_-t}), \quad (\text{A.15})$$

where

$$\omega_\pm = i \frac{\lambda_1^2 + \lambda_2^2}{v} \pm \sqrt{\left(\epsilon + \frac{2\lambda_1\lambda_2}{v} \right)^2 - \left(\frac{\lambda_1^2 + \lambda_2^2}{v} \right)^2} \quad (\text{A.16})$$

Combining this with (A.11) gives

$$z_\infty = - \int_0^\infty dt' \frac{2iT}{\sinh(\pi T t)} \frac{\sqrt{-\omega_+\omega_-}}{\omega_- - \omega_+} (e^{i\omega_+t} - e^{i\omega_-t}), \quad (\text{A.17})$$

which reduces to (22) when the integral is performed.

References

- [1] Moore G and Read N 1991 *Nucl. Phys. B* **360** 362–396
- [2] Greiter M, Wen X G and Wilczek F 1992 *Nucl. Phys. B* **374** 567–614
- [3] Willett R L, Pfeiffer L N and West K W 2009 *PNAS* **106** 8853–8858
- [4] Willett R L, Pfeiffer L N and West K W 2010 *Phys. Rev. B* **82** 205301 (*Preprint arXiv:0911.0345*)
- [5] Fu L and Kane C L 2008 *Phys. Rev. Lett.* **100** 096407 (*Preprint arXiv:0707.1692*)
- [6] Sau J D, Lutchyn R M, Tewari S and Das Sarma S 2010 *Phys. Rev. Lett.* **104** 040502 (*Preprint arXiv:0907.2239*)
- [7] Alicea J 2010 *Phys. Rev. B* **81** 125318 (*Preprint arXiv:0907.2239*)
- [8] Lee P A 2009 (*Preprint arXiv:0907.2681*)
- [9] Kitaev A Y 2003 *Ann. Phys.* **303** 2 (*Preprint quant-ph/9707021*)
- [10] Preskill J 1998 Fault-tolerant quantum computation *Introduction to Quantum Computation* ed Lo H K, Popescu S and Spiller T P (World Scientific) (*Preprint quant-ph/9712048*)
- [11] Freedman M H, Kitaev A, Larsen M J and Wang Z 2003 *Bull. Amer. Math. Soc. (N.S.)* **40** 31–38 ISSN 0273-0979 (*Preprint quant-ph/0101025*)
- [12] Fradkin E, Nayak C, Tsvelik A and Wilczek F 1998 *Nucl. Phys. B* **516** 704–18 (*Preprint cond-mat/9711087*)
- [13] Das Sarma S, Freedman M and Nayak C 2005 *Phys. Rev. Lett.* **94** 166802 (*Preprint cond-mat/0412343*)
- [14] Bonderson P, Shtengel K and Slingerland J K 2006 *Phys. Rev. Lett.* **97** 016401 (*Preprint cond-mat/0601242*)
- [15] Bonderson P, Shtengel K and Slingerland J K 2008 *Ann. Phys.* **323** 2709–2755 (*Preprint arXiv:0707.4206*)
- [16] Akhmerov A R, Nilsson J and Beenakker C W J 2009 *Phys. Rev. Lett.* **102** 216404 (*Preprint arXiv:0903.2196*)
- [17] Fu L and Kane C L 2009 *Phys. Rev. Lett.* **102** 216403 (*Preprint arXiv:0903.2427*)
- [18] Nilsson J and Akhmerov A R 2010 *Phys. Rev. B* **81** 205110 (*Preprint arXiv:0912.4716*)
- [19] Sau J D, Tewari S and Das Sarma S 2010 (*Preprint arXiv:1004.4702*)
- [20] Rosenow B, Halperin B I, Simon S H and Stern A 2008 *Phys. Rev. Lett.* **100** 226803 (*Preprint arXiv:0707.4474*)
- [21] Bishara W and Nayak C 2009 *Phys. Rev. B* **80** 155304 (*Preprint arXiv:0906.0327*)
- [22] Rosenow B, Halperin B I, Simon S H and Stern A 2009 *Phys. Rev. B* **80** 155305 (*Preprint arXiv:0906.0310*)
- [23] Misra B and Sudarshan E C G 1977 *J. Math. Phys.* **18** 756–763
- [24] Milovanović M and Read N 1996 *Phys. Rev. B* **53** 13559–13582 (*Preprint cond-mat/9602113*)
- [25] Fendley P, Fisher M P A and Nayak C 2007 *Phys. Rev. B* **75** 045317 (*Preprint cond-mat/0607431*)
- [26] Volovik G 1999 *JETP Letters* **70**(9) 609–614
- [27] Read N and Green D 2000 *Phys. Rev. B* **61** 10267–10297 (*Preprint cond-mat/9906453*)
- [28] Baraban M, Zikos G, Bonesteel N and Simon S H 2009 *Phys. Rev. Lett.* **103** 076801 (*Preprint http://arxiv.org/abs/0901.3502*)
- [29] Cheng M, Lutchyn R M, Galitski V and Sarma S D 2009 *Phys. Rev. Lett.* **103** 107001 (*Preprint arXiv:0905.0035*)
- [30] Bonderson P 2009 *Phys. Rev. Lett.* **103** 110403 (*Preprint arXiv:0905.2726*)
- [31] Bonderson P, Clarke D J, Nayak C and Shtengel K 2010 *Phys. Rev. Lett.* **104** 180505 (*Preprint arXiv:0911.2691*)
- [32] Clarke D J and Shtengel K 2010 *Phys. Rev. B* **82** 180519 (*Preprint 1009.0302*)